Model reduction for Kuramoto models with complex topologies

Edward J. Hancock[1,2] and Georg A. Gottwald[1]

[1]*School of Mathematics and Statistics, The University of Sydney*
[2]*Charles Perkins Centre, The University of Sydney*

(Dated: April 20, 2018)

Synchronisation of coupled oscillators is a ubiquitous phenomenon, occurring in topics ranging from biology and physics, to social networks and technology. A fundamental and long-time goal in the study of synchronisation has been to find low-order descriptions of complex oscillator networks and their collective dynamics. However, for the Kuramoto model - the most widely used model of coupled oscillators - this goal has remained surprisingly challenging, in particular for finite-size networks. Here, we propose a model reduction framework that effectively captures synchronisation behaviour in complex network topologies. This framework generalises a collective coordinates approach for all-to-all networks [Gottwald (2015) Chaos 25, 053111] by incorporating the graph Laplacian matrix in the collective coordinates. We first derive low dimensional evolution equations for both clustered and non-clustered oscillator networks. We then demonstrate in numerical simulations for Erdős-Rényi (ER) networks that the collective coordinates capture the synchronisation behaviour in both finite-size networks as well as in the thermodynamic limit, even in the presence of interacting clusters.

I. INTRODUCTION

The dynamics of interacting oscillators in complex networks is a ubiquitous model in many fields of science and engineering with examples ranging from the activity of the brain [3, 24] to the functioning of power grids [7]. A hallmark of the observed dynamics is the emergence of collective synchronised behaviour of these oscillators [1, 2, 6, 11, 17, 19, 23]. The prowess of a network to synchronise and the nature of the transition to synchronisation depends strongly on the network topology and on the distribution of the native frequencies. The existence of a synchronised state suggests that it is possible to reduce the complexity of these potentially high-dimensional dynamical systems to just a few degrees of freedom describing the collective behaviour. Recent years have seen some progress in this direction for the widely used Kuramoto model [9, 10, 12, 13, 18, 20, 21]. Most methods, however, assume the case of a network with infinitely many oscillators. Recently, a model reduction based on collective coordinates was introduced which does not rely on the thermodynamic limit [9]. It has since been used to derive optimal synchronisation design strategies and optimal synchrony network topologies [4, 22]. In a stochastic Kuramoto model it allowed for the quantitative description of finite-size effects, in particular the collective diffusion of the mean phase [10]. This collective coordinate approach employs a judiciously chosen ansatz function which approximates the phases of the oscillators as a function of their native frequencies. The temporal evolution of these synchronisation modes is given by the collective coordinates. However, this reduction methodology has only been formulated for the case of all-to-all coupling networks and to annealed complex networks, where averages over network configurations were performed.

In this paper, we propose a model reduction framework that effectively captures synchronisation behaviour in complex network topologies. To do so, we introduce two main advances. First, by incorporating the network's graph Laplacian in the collective coordinate ansatz, we generalise the original approach to complex network topologies. Using the novel ansatz, we derive low dimensional evolution equations for arbitrary network topologies, both for networks with a single synchronised cluster and for networks consisting of several interacting partially synchronised clusters. Second, we present two methods to identify those oscillators which do not participate in the collective behaviour - an issue relevant for intermediate coupling strengths where partial synchronisation occurs. Whereas, identifying those non-participating oscillators was straight forward in the all-to-all coupling network where they are the nodes associated with native frequencies of largest absolute value, this simple rule cannot be extended to arbitrary network topologies. Using the novel ansatz and oscillator identification methods together, we are able to effectively approximate the collective behaviour of finite complex networks with arbitrary topology.

The paper is organised as follows. Section II briefly introduces the Kuramoto model. Section III presents the collective coordinate framework for general network topologies. Section IV presents numerical simulations for Erdős-Rényi networks. We conclude in Section V with a discussion of our results and an outlook.

II. MODEL

A widely used model for the description of interacting oscillators is the Kuramoto model [1, 2, 6, 11, 17, 19, 23, 25]. The Kuramoto model governs the dynamics of the phases φ_i of N interacting phase oscillators with native frequencies ω_i and is given by

$$\dot{\varphi}_i = \omega_i + \frac{K}{N}\sum_{i=1}^{N} a_{ij}\sin(\varphi_j - \varphi_i). \tag{1}$$

Here K denotes the coupling strength and $A = [a_{ij}]$ is the adjacency matrix encoding the topology of the network. We assume here that the network is not directed with a symmetric unweighted adjacency matrix A with $a_{ij} = a_{ji} = 1$ if there is an edge between oscillators i and j, and $a_{ij} = 0$ otherwise.

The degree of a node d_i is then given by $d_i = \sum_j a_{ij}$. We introduce for later the graph Laplacian

$$L = D - A, \tag{2}$$

with degree matrix $D = \mathrm{diag}(d_1, d_2, \cdots, d_N)$. Note that the graph Laplacian of a fully connected network has a single zero-eigenvalue with eigenvector $\mathbf{1}_N$. We assume that the native frequencies are distributed according to some distribution $g(\omega)$ and have, without loss of generality, mean zero, i.e. $\mathbf{1}_N^T \boldsymbol{\omega} = 0$ where $\boldsymbol{\omega} = (\omega_1, \cdots, \omega_N)^T$ denotes the vector of natural frequencies.

Typically, once the coupling strength is sufficiently strong with $K > K_c$ for some critical coupling strength K_c, synchronisation occurs in the sense that the oscillators become locked to their mutual mean frequency $\bar{\Omega} = \frac{1}{N}\sum_{i=1}^N \omega_i$ and their phases become localised about their mean phase [11, 17, 25]. This type of synchronous behaviour is known as global synchronisation and is characterised by a globally attracting manifold on which the dynamics settles [5]. The level of synchronisation is often characterised by the order parameter [11]

$$r(t) = \frac{1}{N}\Big| \sum_{j=1}^N e^{i\varphi_j(t)} \Big|, \tag{3}$$

with $0 \leq r \leq 1$. In practice, the asymptotic limit of this order parameter

$$\bar{r} = \lim_{T\to\infty} \frac{1}{T} \int_{T_0}^{T_0+T} r(t)\, dt, \tag{4}$$

is estimated whereby T_0 is chosen sufficiently large to eliminate transient dynamics.

In the case of full synchronisation with $\varphi_i(t) = \varphi_j(t)$ for all pairs i, j and for all times t we obtain $\bar{r} = r = 1$. In the case where all oscillators behave independently with random initial conditions, $\bar{r} = \mathcal{O}(1/\sqrt{N})$ indicates incoherent phase dynamics; values in between indicate partial coherence.

III. COLLECTIVE COORDINATES

In this section, we generalise the collective coordinates methodology introduced in [9]. We first present the collective coordinate framework for the situation when there is a single cluster of oscillators which tends to mutual synchronisation; we then set out to present the collective coordinate framework which takes into account the situation when several individually but not mutually synchronised clusters interact. In the collective coordinate framework the phases of the N oscillators are expressed via an ansatz function

$$\varphi_i(t) = \Phi_i(\alpha_1(t), \cdots, \alpha_n(t); \omega, A) \tag{5}$$

for $i = 1, \cdots, N$ and $n \ll N$ collective coordinates α_j. The temporal evolution of the N phase variables φ_i is then described by n collective coordinates α_j. This reduces an N dimensional system to an n dimensional one. For all-to-all networks with $a_{ij} = 1$ for all i, j the ansatz $\varphi_i(t) = \Phi_i(t)$ with

$$\Phi_i(t) = \alpha(t)\, \omega_i \tag{6}$$

was proposed in [9]. In the case of a bimodal frequency distribution, which allows for interacting partially synchronised clusters, one has to introduce an additional collective coordinate to capture this interaction. The ansatz (6) was numerically verified and can be motivated in the limit of large coupling strength $K \gg 1$. The Kuramoto model (1) can be cast as $\omega_i = -Kr\sin(\psi - \varphi_i)$ introducing the mean phase ψ [11]. Expanding $\varphi_i = \psi + \arcsin(\omega_i/(rK))$ in $1/K$ for large coupling strength yields up to first order $\varphi_i = \psi + \omega_i/(rK)$. Since the Kuramoto model is invariant under constant phase shifts we may set $\psi = 0$ leading to ansatz (6) with $\psi \equiv 0$ [14]. The evolution equations for the collective coordinates can be determined by minimising the error accrued by restricting the solutions to be of the form (6); the reader is referred to [9] for details.

A. A single synchronising cluster with complex topology

To devise an appropriate ansatz for general network topologies, we again focus on the strongly synchronised state for large K. In the asymptotic limit $K \to \infty$ the globally synchronised state $\varphi_i = \varphi_j = \text{const}$ can be approximated (ignoring a constant mean phase ψ) via linearisation as

$$\boldsymbol{\varphi}_\infty = \frac{N}{K} L^+ \boldsymbol{\omega}, \tag{7}$$

where L^+ denotes the pseudo-inverse of the graph Laplacian (2) (see, for example, [8]). This suggests as an ansatz function with collective coordinate $\bar{\alpha}(t)$

$$\boldsymbol{\varphi} = \boldsymbol{\varphi}_\infty\, (1 + \bar{\alpha}(t)). \tag{8}$$

Introducing $\alpha = 1 + \bar{\alpha}$ and defining

$$\bar{\boldsymbol{\omega}} = \frac{N}{K} L^+ \boldsymbol{\omega}, \tag{9}$$

we propose the ansatz $\varphi_i = \Phi_i$ with

$$\Phi_i = \alpha(t)\, \bar{\omega}_i \tag{10}$$

for $i = 1, \cdots, N$. Note that $L^+\mathbf{1}_N = 0$ and $\mathbf{1}_N^T L^+ \boldsymbol{\omega} = 0$ for any native frequency vector ω. We remark that for all-to-all networks we have $L = NI_n - \mathbf{1}_N\mathbf{1}_N^T$ and the ansatz (10) reduces to the ansatz (6) with α being scaled with $1/K$ [15]. Figure 1 provides a numerical illustration of the validity of the collective coordinate ansatz (10) where we plot the actually observed phases against the collective coordinate ansatz (10) for a small-world network [26] and native frequencies drawn from a normal distribution. The oscillators are clearly well described by the collective coordinate ansatz. The agreement of the phases with the collective coordinate ansatz becomes better for increasing coupling strength. We remark that upon

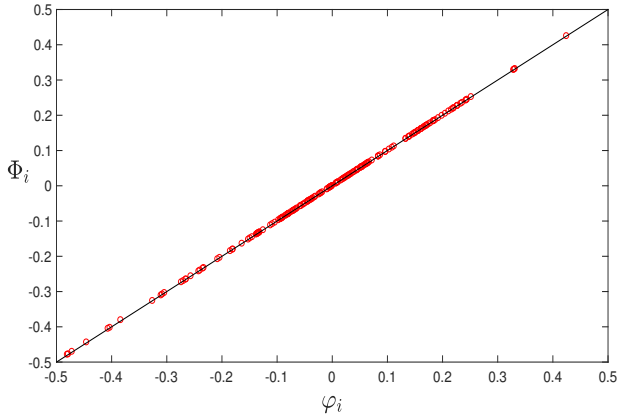

FIG. 1. Snapshot of the phases φ_i obtained form simulating the full Kuramoto model (1) against the collective coordinate ansatz Φ_i (10), with $\alpha = 1.1$ obtained from (11), for a small-world topology with $N = 200$ oscillators, each with 2 neighbours and a rewiring probability $p = 0.3$, and native frequencies drawn from a normal distribution $\mathcal{N}(0, 0.1)$. The corresponding value of the order parameter is $\bar{r} = 0.77$. The continuous line indicates perfect correspondence between the ansatz and the observed phases.

decreasing the coupling strength, not all oscillators are able to synchronise and only a subset of the N oscillators will satisfy the ansatz (10).

We now follow [9] to determine the temporal evolution equations for the collective coordinate α. Inserting the ansatz (10) into the Kuramoto model we obtain the error made by the collective coordinates (10)

$$\mathcal{E}_i = \dot{\alpha}\bar{\omega}_i - \omega_i - \frac{K}{N}\sum_{\substack{j=1\\ j\neq i}} a_{ij}\sin(\alpha(\bar{\omega}_j - \bar{\omega}_i)).$$

We wish to minimise this error, i.e. to maximise the degree to which our collective coordinates are capable of capturing the dynamics of the full Kuramoto model. This is achieved by assuring that the the error is orthogonal to the tangent space of the solution manifold, which is spanned by $\frac{\partial \boldsymbol{\varphi}}{\partial \alpha} = \frac{N}{K} L^{+}\boldsymbol{\omega} = \bar{\boldsymbol{\omega}}$. Setting $\sum_i \mathcal{E}_i\bar{\omega}_i = 0$, we obtain an evolution equation for the collective coordinates

$$\dot{\alpha} = \frac{K}{N}\frac{\bar{\boldsymbol{\omega}}^T L\,\bar{\boldsymbol{\omega}}}{\bar{\boldsymbol{\omega}}^T\bar{\boldsymbol{\omega}}} + \frac{1}{\bar{\boldsymbol{\omega}}^T\bar{\boldsymbol{\omega}}}\frac{K}{N}\sum_{i,j}\bar{\omega}_i a_{ij}\sin(\alpha(\bar{\omega}_j - \bar{\omega}_i)). \quad (11)$$

Upon rescaling time such that $t = T_s\tau$ with

$$T_s = \frac{N}{K}\frac{\bar{\boldsymbol{\omega}}^T\bar{\boldsymbol{\omega}}}{\bar{\boldsymbol{\omega}}^T L\,\bar{\boldsymbol{\omega}}},$$

the evolution equation (11) for the collective coordinate α simplifies to

$$\dot{\alpha} = 1 + \frac{1}{\bar{\omega}^T L\bar{\omega}}\sum_{i,j}\bar{\omega}_i a_{ij}\sin(\alpha(\bar{\omega}_j - \bar{\omega}_i)). \quad (12)$$

Equilibrium solutions $\alpha^\star$ with $\dot{\alpha}^\star = 0$ correspond to the synchronised state and the transition to synchronisation appears at $K = K_c$ which is the smallest K such that (12) supports equilibrium solutions.

Particular choices of frequency distributions or the presence of topological communities within the network, however, may not allow for the global synchronisation of all N oscillators at a given coupling strength N. Instead one observes one or several partially or locally synchronised clusters, with possible complex interactions. One example, already discussed in [9], are Kuramoto models with a unimodal frequency distribution, where the transition to synchronisation is a second-order phase transition [11, 17], and not all oscillators participate in the collective synchronised state. As the coupling strength is increased from zero, at some critical strength $K = K_l$ a few oscillators perform collective behaviour and mutually synchronise. Increasing the coupling strength then allows increasingly more oscillators to become entrained to the synchronised state until global synchronisation sets in at $K = K_c$. Hence for coupling strength $K_l \leq K < K_c$ which allows for local synchronisation we cannot expect to find an equilibrium solution of (12). To capture this local synchronisation for a given coupling strength K within the collective coordinate framework, we assume that all those oscillators that can mutually synchronise will do so. This suggests the ansatz (10) $\varphi_i = \alpha(t)\,\bar{\omega}_i$ for $i \in \mathcal{C}$ where we denote by $\mathcal{C}$ the largest set of nodes which can synchronise. The minimisation of the error then involves only nodes in $\mathcal{C}$ and reads $\sum_{i\in\mathcal{C}}\mathcal{E}_i\bar{\omega}_i = 0$, leading to

$$\dot{\alpha} = 1 + \frac{1}{\bar{\boldsymbol{\omega}}^{(l)T} L_l\,\bar{\boldsymbol{\omega}}^{(l)}}\sum_{i\in\mathcal{C}}\sum_{j\in\mathcal{C}}\bar{\omega}_i a_{ij}\sin(\alpha(\bar{\omega}_j - \bar{\omega}_i)) \quad (13)$$

where we now define

$$\bar{\boldsymbol{\omega}}^{(l)} = \frac{N}{K}L_l^{+}\boldsymbol{\omega}^{(l)}, \quad (14)$$

where $\boldsymbol{\omega}^{(l)}$ denotes the native frequencies of nodes in the set $\mathcal{C}$ and L_l is the graph Laplacian of the network consisting only of nodes in the cluster set $\mathcal{C}$. The set $\mathcal{C}$ is now determined such that its cardinality N_l is determined as the largest possible size such that (13) admits an equilibrium solution $\dot{\alpha}^\star = 0$. In the case of an all-to-all coupling network, this is readily achieved by excluding successively those nodes with native frequencies with the largest absolute frequencies (see [9]). In the case of arbitrary connected complex networks we are not aware of any computationally efficient way to test for the largest set of nodes allowing for stationary equilibrium solutions $\alpha^\star$. We propose here two dynamical criteria to identify those non-entrained nodes by linearising the Kuramoto model (1) about an equilibrium solution $\alpha^\star$ and studying the linearised matrix

$$L_{\text{lin}} = \begin{cases} -a_{ij}\cos(\alpha^\star(\bar{\omega}_j - \bar{\omega}_i)), & i \neq j \\ \sum_k a_{ik}\cos(\alpha^\star(\bar{\omega}_j - \bar{\omega}_i)), & i = j \end{cases}. \quad (15)$$

For a stable system, L_{lin} has one zero eigenvalue and $N-1$ positive eigenvalues. The system becomes unstable when an eigenvalue of L_{lin} becomes negative. For the first criterion,

we assume that the synchronised cluster is comprised of the maximal number of nodes which are able to synchronise in the sense that equilibrium solutions $\alpha^\star$ of (13) exist. For sufficiently large values of the coupling strength K equilibrium solutions can be found corresponding to global synchronisation with $N_l = N$ (note that in this case (13) and (12) are identical). Decreasing the coupling strength K in small increments δK while keeping the number of oscillators fixed for each step, we reach a coupling strength K' such that no equilibrium solution exists. L_{lin} is evaluated around the last equilibrium solution $\alpha^\star$ at $K = K' + \delta K$. The eigenvector $\hat{v}$ of L_{lin} corresponding to the smallest non-zero eigenvalue is then selected to determine the set of nodes to be excluded from the collective coordinate description. In particular, the elements of the eigenvector $\hat{v}$ are ordered and the largest difference or gap between neighbouring elements is determined. The network is then partitioned between those nodes above and below the largest gap, where the group with less elements is discarded. We remark that if this procedure excludes nodes such that the remaining network is disconnected, we choose the largest connected network within this set of nodes. For the second criterion, we identify all nodes which are linearly unstable at a given coupling strength K. As for the first criterion, we use the eigenvector $\hat{v}$ of the linearisation matrix L_{lin} corresponding to the smallest non-zero eigenvalue to determine the set of nodes to be excluded from the collective coordinate description.

In the simulations presented below we simultaneously use both methods of identifying the non-entrained oscillators, which do not partake in the collective behaviour captured by the collective coordinate ansatz. Using the first method, which tests for existence of stationary solutions, provides similar results (not shown). However, we found that including the second method, based on finding the unstable nodes, provides slightly better results, particularly for identifying non-entrained oscillators close to the onset of global synchronisation.

In the following we present the collective coordinate framework when there are more than one locally synchronised cluster.

B. Interacting locally synchronised clusters with complex topology

We now set out to formulate the collective coordinate ansatz allowing for the interaction between several locally synchronised clusters. Let us consider that there are one or several sets of nodes $\mathcal{C}_m$ with $m = 1, \cdots, M$, each of size N_m which exhibit localised collective behaviour within their respective sets. We reformulate the Kuramoto model (1) for the phases of nodes in the mth cluster, $\varphi^{(m)} \in \mathbb{R}^{N_m}$, with native frequencies $\omega_i^{(m)}$ as

$$\dot{\varphi}_i^{(m)} = \omega_i^{(m)} + \frac{K}{N} \sum_{k=1}^{M} \sum_{j \in \mathcal{C}_k} a_{ij} \sin(\varphi_j^{(k)} - \varphi_i^{(m)}), \tag{16}$$

for $i \in \mathcal{C}_m$. To capture the collective behaviour within each set, the collective coordinate approach is then restricted to each set individually. We introduce collective coordinates $\alpha_m(t)$ to describe the collective behaviour within a cluster $\mathcal{C}_m$ and collective mean phase coordinates $f_m(t)$ to account for the interaction between connected clusters $\mathcal{C}_m$ [16]. Analogously to the expansion around the limit $K \to \infty$ in Section III A and the corresponding ansatz for the entire network (10), we propose the ansatz $\boldsymbol{\varphi}^{(m)} = \Phi^{(m)}$ for each cluster $m = 1, \cdots, M$ with

$$\Phi^{(m)} = \bar{\boldsymbol{\omega}}^{(m)} + \bar{\alpha}_m(t)\, \bar{\boldsymbol{\omega}}_c^{(m)} + f_m(t) \mathbf{1}_{N_m}. \tag{17}$$

Here $\bar{\boldsymbol{\omega}}^{(m)}$ is made up of the elements of $\bar{\boldsymbol{\omega}}$ in $\mathcal{C}_m$, and so represents the entire network's asymptotic state. Indeed, for global synchronisation with a single synchronised set of nodes $M = 1$ we have $\bar{\alpha}_1 = 0$ and $f_1 = 0$, and the ansatz (17) reduces to the ansatz (7). We define the asymptotic state of the mth cluster as if it were treated as a single unit disconnected from the rest of the network

$$\bar{\boldsymbol{\omega}}_c^{(m)} = \frac{N}{K} L_m^+ \boldsymbol{\omega}^{(m)}, \tag{18}$$

where $L_m = D_m - A_m$ denotes the Laplacian matrix for the mth cluster with the cluster's adjacency matrix $A_m = [a_{ij}]$ restricted to $i, j \in \mathcal{C}_m$ and associated degree matrix D_m.

Introducing again $\alpha = 1 + \bar{\alpha}$ and defining

$$\bar{\boldsymbol{\omega}}_{c2c}^{(m)} = \bar{\boldsymbol{\omega}}^{(m)} - \bar{\boldsymbol{\omega}}_c^{(m)} \tag{19}$$

we rewrite the ansatz (17) as

$$\Phi^{(m)} = \bar{\boldsymbol{\omega}}_{c2c}^{(m)} + \alpha_m(t)\, \bar{\boldsymbol{\omega}}_c^{(m)} + f_m(t) \mathbf{1}_{N_m}. \tag{20}$$

The collective coordinates $\alpha_m(t)$ describe the internal dynamics of each cluster whereas the collective coordinate $f_m(t)$ describe the interaction between the clusters.

Figure 2 shows a snapshot of the phases for an ER network consisting of two clusters with small inter cluster degree. We show the actual phases obtained from a numerical simulation of the full Kuramoto model (1) and the collective coordinate ansatz (20) for the two clusters. The two clusters are readily identified and the phases are well captured by the collective coordinate ansatz.

Inserting the collective coordinate ansatz (20) into the Kuramoto model (16), we obtain the error for $i \in \mathcal{C}_m$

$$\begin{aligned} \mathcal{E}_i^{(m)} =& \dot{\alpha}_m \bar{\omega}_i^{(m)} + \dot{f}_m - \omega_i^{(m)} \\ & - \frac{K}{N} \sum_{k=1}^{M} \sum_{j \in \mathcal{C}_k} a_{ij} \sin(\Phi_j^{(k)} - \Phi_i^{(m)}). \end{aligned} \tag{21}$$

Again we require the error to be orthogonal to the tangent space of the solution manifold, which is now spanned by $\frac{\partial \boldsymbol{\varphi}^{(m)}}{\partial \alpha_m} = \bar{\boldsymbol{\omega}}_c^{(m)}$ and $\frac{\partial \boldsymbol{\varphi}^{(m)}}{\partial f_m} = \mathbf{1}_{N_m}$. Setting $\sum_{i \in \mathcal{C}_m} \mathcal{E}_i^{(m)} \bar{\omega}_{c_i}^{(m)} = 0$ and $\sum_{i \in \mathcal{C}_m} \mathcal{E}_i^{(m)} = 0$ for all $m = 1, \cdots, M$, this yields the evolution equations for the intracluster collective variable α_m with

$$\begin{aligned} \dot{\alpha}_m =& \frac{K}{N} \frac{\bar{\omega}_c^{(m)^T} L_m \bar{\omega}_c^{(m)}}{\bar{\omega}_c^{(m)^T} \bar{\omega}_c^{(m)}} \\ & + \frac{1}{\bar{\omega}_c^{(m)^T} \bar{\omega}_c^{(m)}} \frac{K}{N} \sum_{k=1}^{M} \sum_{j \in \mathcal{C}_k} \sum_{i \in \mathcal{C}_m} \bar{\omega}_{c_i}^{(m)} a_{ij} \sin(\Phi_j^{(k)} - \Phi_i^{(m)}) \end{aligned} \tag{22}$$

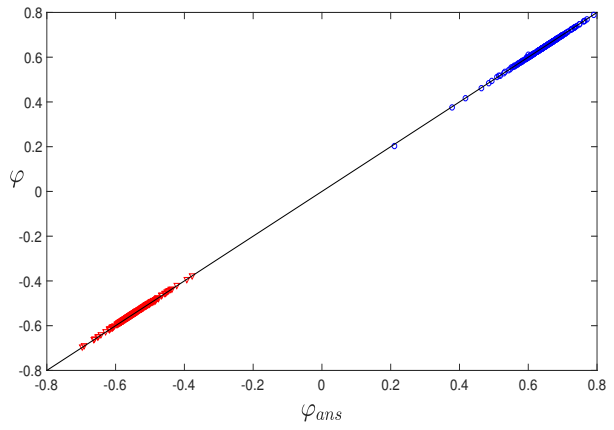

FIG. 2. Snapshot of the phases φ_i obtained form simulating the full Kuramoto model (1) against the collective coordinate ansatz $\Phi_i^{(1,2)}$ (20), with $\alpha_1 = 1.003, \alpha_2 = 1.006, f_1 = -0.095$ obtained from (22) and (23). The network is an ER network with $N = 500$ which consists of two topological clusters. The network is constructed by generating two ER networks, both with a connection probability between two nodes of $p = 0.05$, one with $N_1 = 270$ (triangles) and one with $N_2 = 230$ nodes (open circles), which are then connected via 10 randomly chosen edges. The native frequencies are drawn from a normal distribution $\mathcal{N}(0, 0.02)$. The snapshot is taken at $K = 160$ and the corresponding value of the order parameter is $\bar{r} = 0.83$. The continuous line indicates perfect correspondence between the ansatz and the observed phases.

and for the intercluster variable f_m with

$$\dot{f}_m = \Omega_c^{(m)} + \frac{1}{N_m}\frac{K}{N}\sum_{\substack{k=1\\k\neq m}}^{M}\sum_{j\in C_k}\sum_{i\in C_m} a_{ij}\sin(\Phi_j^{(k)} - \Phi_i^{(m)}), \quad (23)$$

where $\Omega_c^{(m)} = \sum_{i\in C_m}\omega_i^{(m)}/N_m$ is the mean of the native frequencies in the mth cluster. Note that the intercluster collective coordinates satisfy $\sum_{m=1}^{M} N_m f_m = 0$. We remark that for a single cluster $M = 1$ the evolution equations (22)–(23) reduce to (13) with $m = l$ and $\bar{\omega}_c = \bar{\omega}$.

IV. NUMERICAL RESULTS

In the following section we test the methodology on unweighted Erdős-Rényi networks. In an Erdős-Rényi network nodes are connected independently with probability p and where degrees d_j are Poisson-distributed with mean degree $d = pN$. We choose here $p = 0.05$ throughout. We present results for randomly distributed native frequencies, drawn from a distribution $g(\omega)$. In particular, we consider here uniformly distributed native frequencies on the interval $[-1, 1]$ with distribution

$$g(\omega) = 0.5, \quad (24)$$

and normally distributed native frequencies with

$$g(\omega) = \frac{1}{\sqrt{2\pi\sigma_\omega^2}}\exp\left(-\frac{\omega^2}{2\sigma_\omega^2}\right), \quad (25)$$

with $\sigma_\omega^2 = 0.1$.

We begin studying an ER network with uniformly distributed native frequencies. We show in Figure 3 the order parameter $\bar{r}$ as a function of the coupling strength K for two networks with sizes $N = 2000$ and $N = 500$, respectively. The figure shows a comparison of the order parameter as calculated from a long simulation of the full Kuramoto model (1) and as estimated by the collective coordinate ansatz (10) where α is determined as the stationary solution of (12). To solve the collective coordinate evolution equation (12) for stationary solutions $\alpha = \alpha^\star$, we discarded any nodes corresponding to unstable eigenvectors of the linearisation matrix $L_{\rm lin}$ as described in Section III A. Let us denote by C_l the set of nodes for which a linearly stable equilibrium solution $\alpha^\star$ of the collective coordinate can be found. We then calculate the order parameter $\bar{r}$ of the collective coordinate using

$$r_{\rm cc}(t) = \frac{1}{N}\Big|\sum_{j\in C_l} e^{i\alpha^\star\bar{\omega}_j} + \sum_{j\notin C_l} e^{i\omega_j t}\Big|. \quad (26)$$

It is seen in Figure 3 that the collective coordinate approach works very well for the larger network with $N = 2000$ and resolves the explosive transition to synchronisation near $K_c = 26$. The collective coordinate approach identifies the nature of the bifurcation as a saddle-node bifurcation. This is illustrated in Figure 4 where we plot the right-hand-side of the evolution equation (13)

$$\mathcal{F}(\alpha) = 1 + \frac{1}{\bar{\boldsymbol{\omega}}^{(l)T} L_l\, \bar{\boldsymbol{\omega}}^{(l)}}\sum_{i\in C}\sum_{j\in C}\bar{\omega}_i a_{ij}\sin(\alpha(\bar{\omega}_j - \bar{\omega}_i)) \quad (27)$$

as a function of α for coupling strength K below and above the critical coupling strength $K_c = 27$ as well as close to $K = K_c$. Equilibrium solutions are given by $\mathcal{F}(\alpha^\star) = 0$. It is seen that there are no solutions for $K < K_c$ and at $K = K_c$ a pair of equilibrium solutions emerges, one being stable (the smaller one) and one being unstable.

For the smaller network with $N = 500$ nodes, the collective coordinate approach captures the collective synchronisation behaviour very well for large coupling strength K. For smaller coupling strengths with $K < 27$ the match of the order parameters is reasonable; it is seen that the qualitative behaviour is well captured but the functional form, including the concave functional behaviour near $K = 24$, is shifted by $\Delta K \approx 2$.

The delayed synchronisation of the actual Kuramoto model (1), we conjecture, is due to our method not correctly identifying nodes which do not partake in the collective synchronised behaviour captured by the ansatz. This might be due to higher order effects modifying the value of $\Phi_i = \alpha^\star\bar{\omega}_i$ at which $L_{\rm lin}$ is evaluated. Furthermore, we remark that for values of the coupling strength near the onset of synchronisation the interaction between the set of partially synchronised oscillators and the

non-entrained oscillators, which may themselves form small partially synchronised clusters, is not captured by the ansatz (10).

In Figure 5 we present results for normally distributed frequencies. In this case, the order parameter $\bar{r}$ becomes non-zero at some coupling strength $K_l \approx 9$ and a few oscillators with native frequencies close to the mean frequency 0 locally synchronise; increasing the coupling strength allows increasingly more oscillators to synchronise, implying a continuous change of the order parameter as supposed to the hard transition in the case of uniformly distributed native frequencies seen in Figure 3. At some coupling strength $K_c \approx 16$, global synchronisation sets in affecting all oscillators. The normalised domain length L_{domain}, as calculated from the collective coordinate approach, is depicted in Fig 6 and shows a smooth transition from $L_{\text{domain}} = 0$ to $L_{\text{domain}} = 1$ for the larger network, corresponding to the larger and larger number of oscillators joining the single synchronised cluster.

As for the cases of the uniformly distributed native frequencies, the larger network's dynamics is very well described by the collective coordinate ansatz (10) capturing both, the local and the global synchronisation. The smaller network with $N = 500$ nodes has a larger error describing the synchronisation behaviour accurately near the onset at $K = K_l$. This is due to, we conjecture, the presence of interacting clusters which form upon decreasing the coupling strength. In each of these smaller clusters, nodes locally synchronise and then interact. This is not described by the ansatz (10).

In Figure 6 we show the normalised domain length

$$L_{\text{domain}} = \frac{N_l}{N}, \tag{28}$$

where N_l is the size of the network after discarding the unstable nodes, i.e. the size of $\mathcal{C}_l$, based on the linearisation matrix L_{lin} as described in Section III A. One sees clearly the gradual increase of the size of the synchronised cluster with increasing coupling strength describing the local synchronisation behaviour. We show results for the larger network with $N = 2000$; the plot for the smaller network looks similar (not shown).

In the remainder we show that the collective coordinate ansatz (20), is able to capture the interacting dynamics of localised clusters. In order to do so we consider an artificial ER network which is prepared to allow for two well-specified topological clusters. We show here that, once clusters are identified, the collective coordinate framework is able to describe their dynamics and their interaction. We consider an ER network with $N = 500$ nodes. The network is constructed by generating two ER networks, both with a connection probability between two nodes of $p = 0.05$, one with $N_1 = 270$ and one with $N_2 = 230$ nodes. The two clusters are then linked by 10 randomly chosen edges. In this case the clusters can be identified by the smallest non-zero (positive) eigenvalue and corresponding eigenvector of L_{lin} in (15). We remark, however, that in general the identification of clusters is a nontrivial task that is not the focus of this work. We consider again native frequencies drawn from a normal distribution $\mathcal{N}(0, 0.02)$ allowing for local synchronisation within each cluster of oscillators with small absolute native frequencies. Figure 7 shows the order parameter $\bar{r}$ as calculated from a long simulation of the full Kuramoto model (1) and for the collective coordinate approach. The full simulation reveals the following synchronisation behaviour of this particular clustered network: At $K \approx 9$ the two topological clusters individually begin to locally synchronise (cf. Figure 5). Between $50 < K \leq 142$, both clusters are synchronised and the coupling is not strong enough to allow the two clusters to interact. In this range the order parameter is well approximated by

$$\begin{aligned}\bar{r} &= \frac{\Delta\omega}{2\pi}\int_0^{\frac{\Delta\omega}{2\pi}} \Big|\sum_{j\in C_1} e^{i\varphi_j} + \sum_{j\in C_s} e^{i\varphi_j}\Big|\, dt \\ &\approx \frac{\Delta\omega}{2\pi}\int_0^{\frac{\Delta\omega}{2\pi}} \frac{1}{N}\sqrt{N_1^2 + N_2^2 + 2N_1N_2\cos(\Delta\omega t)}\, dt \\ &\approx 0.64,\end{aligned}$$

where $\Delta\omega = 0.023$ is the difference in the mean frequencies of the two respective clusters. Increasing the coupling strength past $K = 142$ the clusters are interacting and increasing K

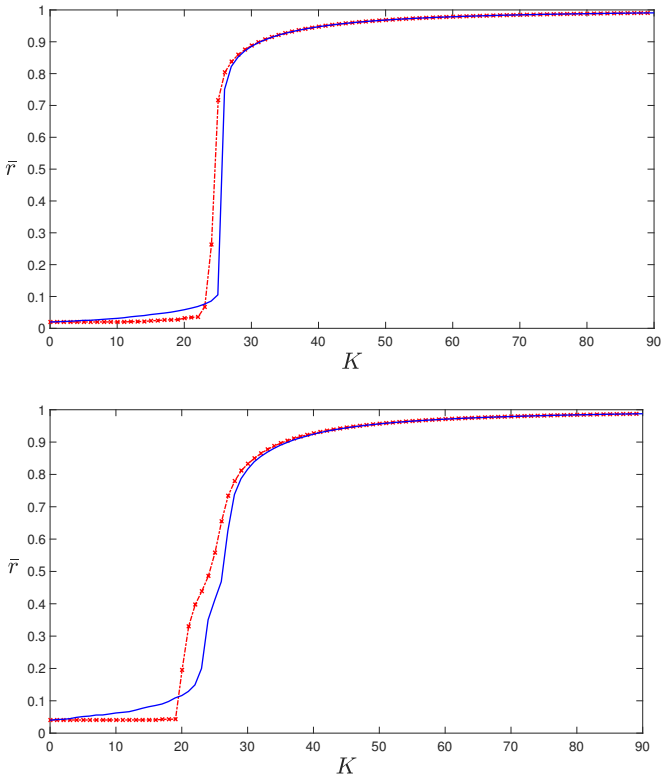

FIG. 3. Order parameter $\bar{r}$ as a function of the coupling strength K for an ER network with uniformly distributed native frequencies. Depicted are results from a direct numerical integration of the Kuramoto model (1) (continuous line, online blue) and from the collective coordinate approach (10) using (26) (crosses, online red). Top: ER network with $N = 2000$ nodes. Bottom: ER network with $N = 500$ nodes.

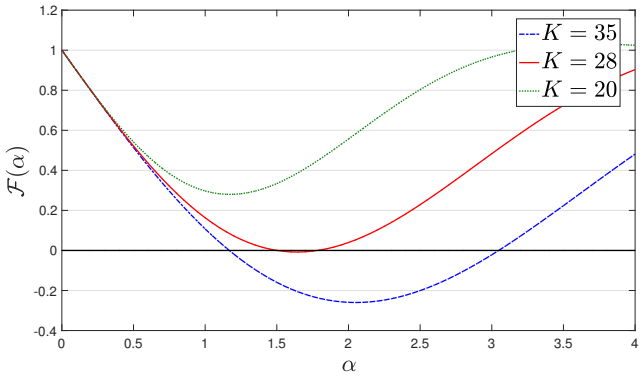

FIG. 4. Right-hand-side $\mathcal{F}(\alpha)$ of the evolution equation (13) for several values of K for the $N = 500$ ER network with uniformly distributed native frequencies with a subcritical coupling strength $K = 20 < K_c$, critical coupling strength $K = 28 \approx K_c$ and supercritical coupling strength $K = 35 > K_c$. Parameters as in Figure 3.

eventually leads to global synchronisation.

This path to synchronisation involving interacting clusters is remarkably well described by the collective coordinate ansatz. Starting at large values of the coupling strength the ansatz for two interacting clusters (20) with $\alpha_{1,2}$ and f determined by solving (22)–(23) captures the interaction between the clusters remarkably well. At $K \approx 142$ the collective coordinate solution becomes linearly unstable; the eigenvector $\hat{v}$ of the linearisation matrix L_{lin} corresponding to this instability consists of two separated parts identifying accurately the two topological clusters of the network. For $K \leq 142$ the two clusters can be described each by the single-cluster ansatz (10), each with their own independent collective coordinate α. The stationary solutions of the evolution equation (13) for the respective collective coordinates and the associated order parameter reproduces very well the collective behaviour of the full finite-size Kuramoto model.

V. DISCUSSION AND OUTLOOK

We derived a collective coordinate approach for interacting Kuramoto oscillators on arbitrary networks. Our approach allows for the description of finite size networks away from the thermodynamic limit and is capable of describing the interaction of partially synchronised interacting clusters. We remark that when approaching the onset of synchronisation from large coupling strength in the case of normally distributed frequencies, for which we observe local synchronisation, the number of partially synchronised clusters typically will grow and near onset of synchronisation the collective coordinate approach might be computationally as costly as simulating the full system.

Here we identified clusters for a very clear clustering example. This is, of course, in general not the case. It is a highly non-trivial and, to our knowledge, an unsolved task to identify clusters for fixed coupling strength K. Clusters are formed in an intricate interplay between the network topology and the distribution of the native frequencies. In our study of two interacting clusters we found that the linearisation matrix L_{lin} (which incorporates information about the network topology and the native frequencies) was able to identify the coupling strength for which clusters start to interact. Whether the linearisation matrix is able to identify clusters in more complex cases will be studied in further research.

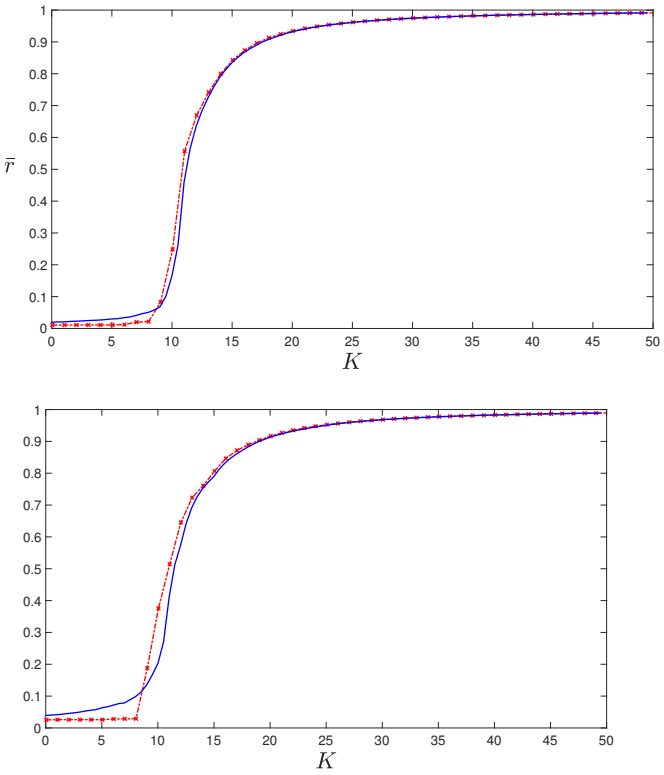

FIG. 5. Order parameter $\bar{r}$ as a function of the coupling strength K for an ER network with normally distributed native frequencies. Depicted are results from a direct numerical integration of the Kuramoto model (1) (continuous line, online blue) and from the collective coordinate approach (10) using (26) (crosses, online red). Top: ER network with $N = 2000$ nodes. Bottom: ER network with $N = 500$ nodes.

ACKNOWLEDGMENTS

GAG acknowledges support from the Australian Research Council, grant DP180101991. EJH gratefully acknowledges the donation from Judith and David Coffey.

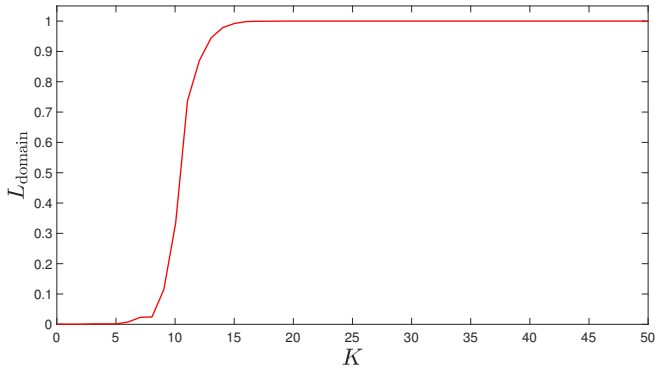

FIG. 6. Normalised domain length L_{domain} as a function of the coupling strength K for the ER networks depicted in Figure 5 with $N = 2000$ nodes and normally distributed native frequencies.

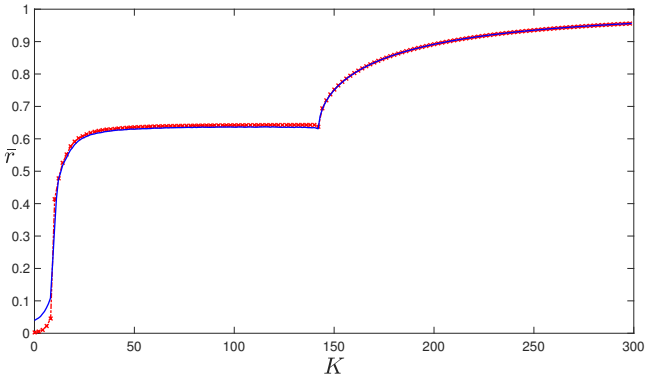

FIG. 7. Order parameter $\bar{r}$ as a function of the coupling strength K for an ER network consisting of two coupled topological clusters with normally distributed native frequencies. The network is the same as that used for Figure 2. Depicted are results from a direct numerical integration of the Kuramoto model (1) (continuous line, online blue) and from the collective coordinate approach (10) using (26) (crosses, online red).

[1] Juan A. Acebrón, L. L. Bonilla, Conrad J. Pérez Vicente, Félix Ritort, and Renato Spigler. The Kuramoto model: A simple paradigm for synchronization phenomena. *Rev. Mod. Phys.*, 77:137–185, Apr 2005.

[2] Alex Arenas, Albert Diaz-Guilera, Jürgen Kurths, Yamir Moreno, and Changsong Zhou. Synchronization in complex networks. *Phys. Rep.*, 469(3):93–153, 2008.

[3] D. Bhowmik and M. Shanahan. How well do oscillator models capture the behaviour of biological neurons? In *The 2012 International Joint Conference on Neural Networks (IJCNN)*, pages 1–8, 2012.

[4] Markus Brede and Alexander C. Kalloniatis. Frustration tuning and perfect phase synchronization in the Kuramoto-Sakaguchi model. *Phys. Rev. E*, 93:062315, Jun 2016.

[5] John David Crawford. Amplitude expansions for instabilities in populations of globally-coupled oscillators. *Journal of Statistical Physics*, 74(5-6):1047–1084, 1994.

[6] Florian Dörfler and Francesco Bullo. Synchronization in complex networks of phase oscillators: A survey. *Automatica*, 50(6):1539 – 1564, 2014.

[7] G. Filatrella, A. H. Nielsen, and N. F. Pedersen. Analysis of a power grid using a Kuramoto-like model. *The European Physical Journal B*, 61(4):485–491, Feb 2008.

[8] G. H. Golub and Ch. F. Van Loan. *Matrix Computations*. The Johns Hopkins University Press, Baltimore, 3rd edition, 1996.

[9] Georg A. Gottwald. Model reduction for networks of coupled oscillators. *Chaos*, 25(5):053111, 12, 2015.

[10] Georg A. Gottwald. Finite-size effects in a stochastic Kuramoto model. *Chaos: An Interdisciplinary Journal of Nonlinear Science*, 27(10):101103, 2017.

[11] Y. Kuramoto. *Chemical Oscillations, Waves, and Turbulence*, volume 19 of *Springer Series in Synergetics*. Springer-Verlag, Berlin, 1984.

[12] E. A. Martens, E. Barreto, S. H. Strogatz, E. Ott, P. So, and T. M.

Antonsen. Exact results for the Kuramoto model with a bimodal frequency distribution. *Phys. Rev. E*, 79:026204, Feb 2009.

[13] Seth A. Marvel, Renato E. Mirollo, and Steven H. Strogatz. Identical phase oscillators with global sinusoidal coupling evolve by Möbius group action. *Chaos*, 19(4):043104, 11, 2009.

[14] For stochastic Kuramoto models, the mean phase experiences non-trivial diffusive behaviour which can also be captured by the collective coordinate framework, see [10].

[15] Note that L has a single zero eigenvalue with corresponding eigenvector V_1 satisfying $V_1^T\omega = 0$, and $N-1$ repeated eigenvalues $\lambda = N$. Using an eigenvalue decomposition, write $L^+\omega = V D^+ V^T\omega = \lambda^{-1}\omega$ which implies (6).

[16] See [9] for an example of two interacting clusters in an all-to-all coupling network with a bimodal frequency distribution.

[17] Grigory V. Osipov, Jürgen Kurths, and Changsong Zhou. *Synchronization in Oscillatory Networks*. Springer Series in Synergetics. Springer, Berlin, 2007.

[18] Edward Ott and Thomas M. Antonsen. Low dimensional behavior of large systems of globally coupled oscillators. *Chaos*, 18(3):037113, 6, 2008.

[19] A Pikovsky, M. Rosenblum, and J. Kurths. *Synchronization: A Universal Concept in Nonlinear Sciences*. Cambridge University Press, Cambridge, 2001.

[20] Arkady Pikovsky and Michael Rosenblum. Partially integrable dynamics of hierarchical populations of coupled oscillators. *Phys. Rev. Lett.*, 101:264103, Dec 2008.

[21] Arkady Pikovsky and Michael Rosenblum. Dynamics of heterogeneous oscillator ensembles in terms of collective variables. *Physica D*, 240(9–10):872 – 881, 2011.

[22] Rafael S. Pinto and Alberto Saa. Optimal synchronization of Kuramoto oscillators: a dimensional reduction approach. *Phys. Rev. E (3)*, 92(6):062801, 6, 2015.

[23] Francisco A. Rodrigues, Thomas K. DM. Peron, Peng Ji, and Jürgen Kurths. The Kuramoto model in complex networks. *Physics Reports*, 610:1 – 98, 2016.

[24] Jane H. Sheeba, Aneta Stefanovska, and Peter V. E. McClintock. Neuronal synchrony during anesthesia: A thalamocortical model. *Biophysical Journal*, 95(6):2722–2727, 2008.

[25] Steven H. Strogatz. From Kuramoto to Crawford: Exploring the onset of synchronization in populations of coupled oscillators. *Physica D*, 143(1-4):1–20, 2000.

[26] Duncan J. Watts and Steven H. Strogatz. Collective dynamics of 'small-world' networks. *Nature*, 393:440 EP –, 06 1998.